Plenary address delivered at ICM 2002
International Congress of Mathematicians
Beijing, China, August 24, 2002

Differential complexes and numerical stability

Douglas N. Arnold*

January 20, 2003

Abstract

Differential complexes such as the de Rham complex have recently come to play an important role in the design and analysis of numerical methods for partial differential equations. The design of stable discretizations of systems of partial differential equations often hinges on capturing subtle aspects of the structure of the system in the discretization. In many cases the differential geometric structure captured by a differential complex has proven to be a key element, and a discrete differential complex which is appropriately related to the original complex is essential. This new geometric viewpoint has provided a unifying understanding of a variety of innovative numerical methods developed over recent decades and pointed the way to stable discretizations of problems for which none were previously known, and it appears likely to play an important role in attacking some currently intractable problems in numerical PDE.

2000 Mathematics Subject Classification: 65N12.
Keywords and Phrases: finite element, numerical stability, differential complex

1. Introduction

During the twentieth century chain complexes, their exactness properties, and commutative diagrams involving them pervaded many branches of mathematics, most notably algebraic topology and differential geometry. Recently such homological techniques have come to play an important role in a branch of mathematics often thought quite distant from these, numerical analysis. Their most significant applications have been to the design and analysis of numerical methods for the solution of partial differential equations.

Let us consider a general problem, such as a boundary value problem in partial differential equations, as an operator equation: given data f in some space Y find

*Institute for Mathematics and its Applications, University of Minnesota, 400 Church St. S.E., Minneapolis, MN 55455, USA. E-mail: arnold@ima.umn.edu

the solution u in some space X to the problem $Lu = f$. A numerical method discretizes this problem through the construction of an operator $L_h : X_h \to Y_h$ and data $f_h \in Y_h$ and defines an approximate solution $u_h \in X_h$ by the equation $L_h u_h = f_h$. Of course the numerical method is not likely to be of value unless it is consistent which means that L_h and f_h should be close to L and f in an appropriate sense.

Before we speak of solving the original problem, numerically or otherwise, we should first confront the question of whether it is well-posed. That is, given $f \in Y$, does a unique $u \in X$ exist, and, if so, do small changes of f induce small changes in Y? The analogous questions for the numerical method, whether given $f_h \in Y_h$ a unique $u_h \in X_h$ is determined by the discrete equation $L_h u_h = f_h$, and whether small changes in f_h induce small changes in u_h, is the question of *stability* of the numerical method. A common paradigm, which can be formalized in many contexts of numerical analysis, is that a method which is consistent and stable is convergent.

Well-posedness is a central issue in the theory of partial differential equations. Of course, we do not expect just any PDE problem to be well-posed. Well-posedness hinges on structure of the problem which may be elusive or delicate. Superficially small changes, for example to the sign of a coefficient or the type of boundary conditions, can certainly destroy well-posedness. The same is true for the stability of numerical methods: it often depends on subtle or elusive properties of the numerical scheme. Usually stability reflects some portion of the structure of the original problem that is captured by the numerical scheme. However in many contexts it is not enough that the numerical scheme be close to the original problem in a quantitative sense for it to inherit stability. That is, it may well happen that a consistent method for a well-posed problem is unstable. In this paper we shall see several examples where the exactness properties of discrete differential complexes and their relation to differential complexes associated with the PDE are crucial tools in establishing the stability of numerical methods. In some cases the homological arguments have served to elucidate or validate methods that had been developed over the preceding decades. In others they have pointed the way to stable discretizations of problems for which none were previously known. They will very likely play a similar role in the eventual solution of some formidable open problems in numerical PDE, especially for problems with significant geometric content, such as in numerical general relativity. As in other branches of mathematics, in numerical analysis differential complexes serve both to encode key structure concisely and to unify considerations from seemingly very different contexts.

In this paper we shall discuss only finite element methods since, of the major classes of numerical methods for PDE, they are the most amenable to rigorous analysis, and have seen the greatest use of differential complexes. But complexes have recently arisen in the study of finite differences, finite volumes, and spectral methods as well.

2. Finite element spaces

A finite element space on a domain Ω is a function space defined piecewise by a certain assembly procedure which we now recall; cf. [7]. For simplicity, here we shall restrict to spaces of piecewise polynomials with respect to a triangulation of an n-dimensional domain by n-simplices with $n = 2$ or 3 (so implicitly we are assuming that $\Omega \subset \mathbb{R}^2$ is polygonal or $\Omega \subset \mathbb{R}^3$ is polyhedral). On each simplex T we require that there be given a function space of *shape function* W_T and a set of *degrees of freedom*, i.e., a set of linear functionals on W_T which form a basis for the dual space. Moreover, each degree of freedom is supposed to be associated with a some subsimplex of some dimension, i.e., in three dimensions with a vertex, an edge, a face, or the tetrahedron itself. For a subsimplex which is shared by two simplices in the triangulation, we assume that the corresponding functionals are in one-to-one-correspondence. Then the finite element space W_h is defined as those functions on Ω whose restriction to each simplex T of the triangulation belongs to W_T and for which the corresponding degrees of freedom agree whenever a subsimplex is shared by two simplices.

The simplest example is obtained by choosing W_T to be the constant functions and taking as the only degree of freedom on T the 0th order moment $\phi \mapsto \int_T \phi(x)\,dx$ (which we associate with T itself). The resulting finite element space is simply the space of piecewise constant functions with respect to the given triangulation. Similarly we could choose $W_T = \mathbb{P}_1(T)$ (by $\mathbb{P}_p(T)$ we denote the space of polynomial functions on T of degree at most p), and take as degrees of freedom the moments of degrees 0 and also those of degree 1, $\phi \mapsto \int_T \phi(x)x_i\,dx$. Again all the degrees of freedom are associated to T itself. This time the finite element space consists of all piecewise linear functions. Of course, the construction extends to higher degrees.

A more common piecewise linear finite element space occurs if we again choose $W_T = \mathbb{P}_1(T)$, but take as degrees of freedom the maps $\phi \mapsto \phi(v)$, one associated to each vertex v. In this case the assembled finite element space consists of all *continuous* piecewise linear functions. More generally we can choose $W_T = \mathbb{P}_p(T)$ for $p \geq 1$, and associate to each vertex the evaluation degrees of freedom just mentioned, to each edge the moments on the edge of degree at most $p-2$, to each face the moments on the face of degree at most $p-3$, and to each tetrahedron the moments of degree at most $p-4$. The resulting finite element space, called the *Lagrange finite element* of degree p, consists of all continuous piecewise polynomials of degree at most p. Figure 1 shows a mesh of a two dimensional domain and a typical function in the space of Lagrange finite elements of degree 2 with respect to this mesh.

Mnemonic diagrams as in Figure 2 are often associated to finite element spaces, depicting a single element T and a marker for each degree of freedom.

Next we describe some finite element spaces that can be used to approximate vector-valued functions. For brevity we limit the descriptions to the 3-dimensional case, but supply diagrams in both 2 and 3 dimensions. Of course we may simply take the Cartesian product of three copies of one of the previous spaces. For example, the element diagrams shown on the left of Figure 3 refer to continuous piecewise linear vector fields in two and three dimensions. More interesting spaces are the

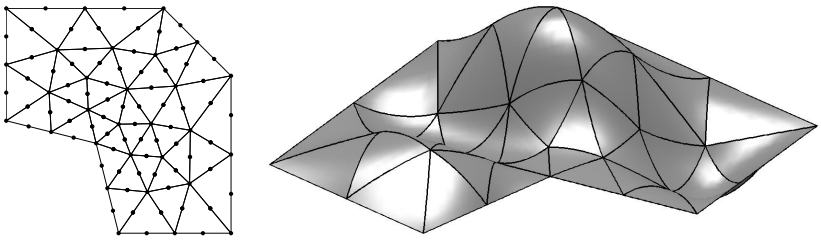

Figure 1: A mesh marked with the locations of the degrees of freedom of for Lagrange finite elements of degree 2 and a typical such finite element function.

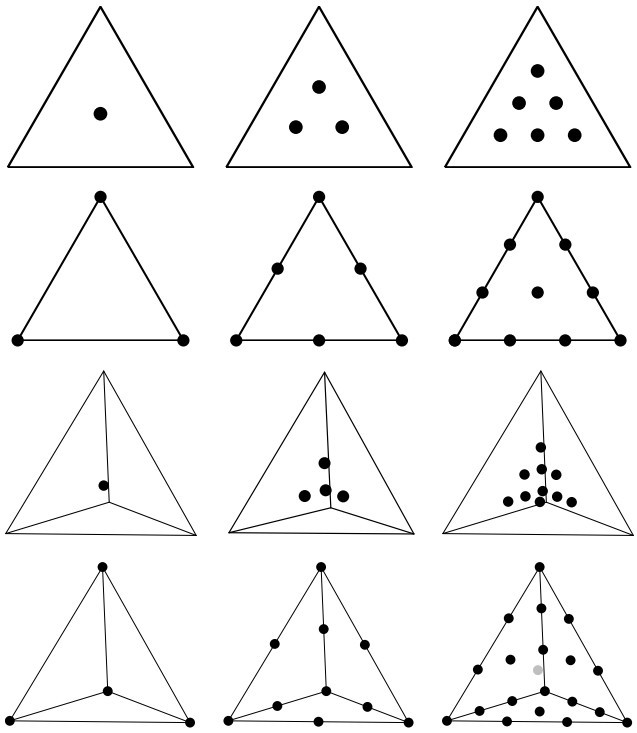

Figure 2: Element diagrams. First row: discontinuous elements of degrees 0, 1, and 2 in two dimensions. Second row: Lagrange elements of degrees 1, 2, and 3 in two dimensions. Third and fourth rows: the corresponding elements in three dimensions.

face elements and *edge elements* essentially conceived by Raviart and Thomas [12] in two dimensions and by Nedelec [10] in three dimensions. In the lowest order case, the face elements take as shape functions polynomial vector fields of the form $p(x) = a + bx$ where $a \in \mathbb{R}^3$, $b \in \mathbb{R}$ and $x = (x_1, x_2, x_3)$, a 4-dimensional subspace of the 12-dimensional space $\mathbb{P}_1(T, \mathbb{R}^3)$ of polynomial vector fields of degree at most

1. The degrees of freedom are taken to be the 0th order moments of the normal components on the faces of codimension 1, $p \mapsto \int_f p(x) \cdot n_f \, dx$ where f is a face and n_f the unit normal to the face. The element diagram is shown in the middle column of Figure 3. In the lowest order case the edge elements shape functions are polynomial vector fields of the form $p(x) = a + b \times x$ where $a, b \in \mathbb{R}^3$, which form a 6-dimensional subspace of $\mathbb{P}_1(T, \mathbb{R}^3)$. The degrees of freedom are the 0th order moments over the edges of the component tangent to the edge, $p \mapsto \int_e p(x) \cdot t_e \, dx$, as indicated on the right of Figure 3.

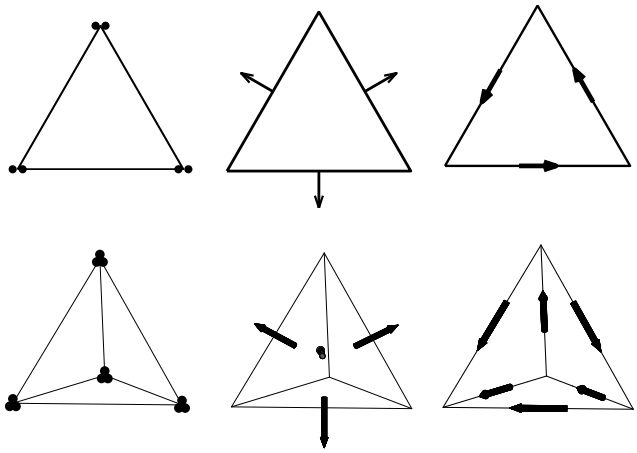

Figure 3: Element diagrams for some finite element approximations to vector fields in two and three dimensions. Multiple dots are used as markers to indicate the evaluation of all components of a vector field. Arrows are used for normal moments on codimension 1 subsimplices and for tangential components on edges. Left: continuous piecewise linear fields. Middle: face elements of lowest order. Right: edge elements of lowest order.

Each of these spaces can be generalized to arbitrarily high order. For the next higher order face space, the shape functions take the form $p(x) = a(x) + b(x)x$ where $a \in \mathbb{P}_1(T, \mathbb{R}^3)$ and $b \in \mathbb{P}_1(T)$ a linear scalar-valued polynomial. This gives a subspace of $\mathbb{P}_2(T, \mathbb{R}^3)$ of dimension 15, and the degrees of freedom are the moments of degree at most 1 of the normal components on the faces and the moments of degree 0 of all components on the tetrahedron. This element is indicated on the left of Figure 4. For the second lowest order edge space, the shape functions take the form $p(x) = a(x) + b(x) \times x$ with $a, b \in \mathbb{P}_1(T, \mathbb{R}^3)$, giving a 20-dimensional space. The degrees of freedom are the tangential moments of degree at most 1 on the edges (two per edge) and the tangential moments of degree 0 on the faces (two per face). This element is indicated on the right of Figure 4.

The choice of the shape functions and the degrees of freedom determine the smoothness of the functions belonging to the assembled finite element space. For example, the Lagrange finite element spaces of any degree belong to the Sobolev space $H^1(\Omega)$ of $L^2(\Omega)$ functions whose distributial first partial derivatives also belong to

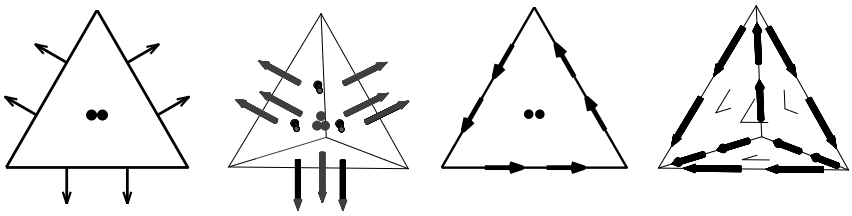

Figure 4: The face (left) and edge (right) elements of the second lowest order in 2- and 3-dimensions.

$L^2(\Omega)$ (and even to $L^\infty(\Omega)$). In fact, the distributional first partial derivative of a continuous piecewise smooth function coincides with its derivative taken piecewise and so belongs to L^2. Thus the degrees of freedom we imposed in constructing the Lagrange finite elements are sufficient to insure that the assembled finite element space $W_h \subset H^1(\Omega)$. In fact more is true: for the Lagrange finite element space with shape function spaces $W_T = \mathbb{P}_p(T)$, we have

$$W_h = \{\, u \in H^1(\Omega) \,|\, u|_T \in W_T \text{ for all simplices } T \text{ of the triangulation} \,\}.$$

This says that, in a sense, the degrees of freedom impose exactly the continuity required to belong to H^1, no less and no more.

In contrast, the discontinuous piecewise polynomial spaces are subsets of $L^2(\Omega)$ but not of $H^1(\Omega)$, since their distributional first derivatives involve distributions supported on the interelement boundaries, and so do not belong to $L^2(\Omega)$.

For the vector-valued finite elements there are more possibilities. The face and edge spaces contain discontinuous functions, and so are not contained in $H^1(\Omega, \mathbb{R}^3)$. However, for vector fields belonging to one of the face spaces the normal component of the vector field does not jump across interelement boundaries, and this implies, via integration by parts, that the distributional divergence of the function coincides with the divergence taken piecewise. Thus the face spaces belong to $H(\mathrm{div}, \Omega)$, the space of L^2 vector fields on Ω whose divergence belongs to L^2. Indeed, for these spaces the degrees of freedom impose exactly the continuity of $H(\mathrm{div})$, no less or more. For the edge spaces it can be shown that the tangential components of a vector field do not jump across element boundaries, and this implies that the edge functions belong to $H(\mathrm{curl}, \Omega)$, the space of L^2 vector fields whose curl belongs to L^2. Again the degrees of freedom impose exactly the continuity needed for inclusion in $H(\mathrm{curl})$.

3. Discrete differential complexes

The de Rham complex

$$\mathbb{R} \hookrightarrow \bigwedge{}^0(\Omega) \xrightarrow{d} \bigwedge{}^1(\Omega) \xrightarrow{d} \cdots \xrightarrow{d} \bigwedge{}^n(\Omega) \to 0$$

is defined for an arbitrary smooth n-manifold Ω. Here $\bigwedge^k(\Omega)$ denotes the space of differential k-forms on Ω, i.e., for $\omega \in \bigwedge^k(\Omega)$ and $x \in \Omega$, $\omega(x)$ is an alternating k-

linear map on the tangent space $T_x\Omega$. The operators $d : \bigwedge^k(\Omega) \to \bigwedge^{k+1}(\Omega)$ denotes exterior differentiation. This is is a complex in that the composition of two exterior differentiations always vanishes, and if the manifold is topologically trivial, then it is exact.

If Ω is a domain in $\mathbb{R}^3$, then we may identify its tangent space at any point with $\mathbb{R}^3$. Using the Euclidean inner product, the space of linear maps on $\mathbb{R}^3$ may be identified by $\mathbb{R}^3$ as usual, so $\bigwedge^1(\Omega)$ may be identified with the space $C^\infty(\Omega, \mathbb{R}^3)$ of smooth vector fields on Ω. Moreover, the space of alternating bilinear maps on $\mathbb{R}^3$ may be identified with $\mathbb{R}^3$ by associating to a vector u the alternating bilinear map $(v, w) \mapsto \det(u|v|w)$. Thus we have an identification of $\bigwedge^2(\Omega)$ with $\mathbb{R}^3$ as well. Finally the only alternating trilinear maps on $\mathbb{R}^3$ are given by multiples of the determinant map $(u, v, w) \mapsto c \det(u|v|w)$, and so we may identify $\bigwedge^3(\Omega)$ with $C^\infty(\Omega)$. In terms of such *proxy fields*, the de Rham complex becomes

$$\mathbb{R} \hookrightarrow C^\infty(\Omega) \xrightarrow{\text{grad}} C^\infty(\Omega, \mathbb{R}^3) \xrightarrow{\text{curl}} C^\infty(\Omega, \mathbb{R}^3) \xrightarrow{\text{div}} C^\infty(\Omega, \mathbb{R}) \to 0. \tag{3.1}$$

Alternatively we may consider L^2-based forms and the sequence becomes

$$\mathbb{R} \hookrightarrow H^1(\Omega) \xrightarrow{\text{grad}} H(\text{curl}, \Omega) \xrightarrow{\text{curl}} H(\text{div}, \Omega) \xrightarrow{\text{div}} L^2(\Omega, \mathbb{R}) \to 0.$$

The finite element spaces constructed above allow us to form discrete analogues of the de Rham complex. Given some triangulation of $\Omega \subset \mathbb{R}^3$, let W_h denote the space of continuous piecewise linear finite elements, Q_h the lowest order edge element space, S_h the lowest order face element space, and V_h the space of piecewise constants. Then $\operatorname{grad} W_h \subset Q_h$ (since Q_h contains all piecewise constant vector fields belonging to $H(\text{curl})$ and the gradient of a continuous piecewise linear is certainly such a function), $\operatorname{curl} Q_h \subset S_h$ (since S_h contains all piecewise constant vector fields belonging to $H(\text{curl})$), and $\operatorname{div} S_h \subset V_h$. Thus we have the discrete differential complex

$$\mathbb{R} \hookrightarrow W_h \xrightarrow{\text{grad}} Q_h \xrightarrow{\text{curl}} S_h \xrightarrow{\text{div}} V_h \to 0. \tag{3.2}$$

This differential complex captures the topology of the domain to the same extent as the de Rham complex. In particular, if the domain is topologically trivial, then the sequence is exact.

It is convenient to abbreviate the above statement using the element diagrams introduced earlier. Thus we will say that the following complex is exact:

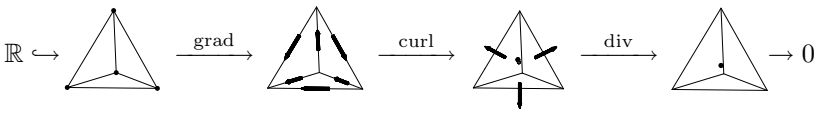

By this we mean that if we assemble finite element spaces W_h, Q_h, S_h, and V_h using the indicated finite elements and a triangulation of a topologically trivial domain, then the corresponding discrete differential complex (3.2) is exact.

There is another important relationship between the de Rham complex (3.1) and the discrete complex (3.2). The defining degrees of freedom determine projections $\Pi_h^W : C^\infty(\Omega) \to W_h$, $\Pi_h^Q : C^\infty(\Omega, \mathbb{R}^3) \to Q_h$, and so on. In fact Π_h^W is

just the usual interpolant, Π_h^V is the L^2-projection into the piecewise constants, and the projections Π_h^Q and Π_h^S onto the edge and face elements are determined by the maintenance of the appropriate moments. It can be checked, based on Stokes theorem, that the following diagram commutes.

$$\begin{array}{ccccccccc}
\mathbb{R} \hookrightarrow & C^\infty(\Omega,\mathbb{R}) & \xrightarrow{\text{grad}} & C^\infty(\Omega,\mathbb{R}^3) & \xrightarrow{\text{curl}} & C^\infty(\Omega,\mathbb{R}^3) & \xrightarrow{\text{div}} & C^\infty(\Omega,\mathbb{R}) & \to 0 \\
& \downarrow \Pi_h^W & & \downarrow \Pi_h^Q & & \downarrow \Pi_h^S & & \downarrow \Pi_h^V & \\
\mathbb{R} \hookrightarrow & W_h & \xrightarrow{\text{grad}} & Q_h & \xrightarrow{\text{curl}} & S_h & \xrightarrow{\text{div}} & V_h & \to 0
\end{array} \tag{3.3}$$

The finite element spaces appearing in this diagram, with one degree of freedom for each vertex for W_h, for each edge for Q_h, for each face for S_h, and for each simplex for V_h, are highly geometrical. In fact, recalling the identifications between fields and differential forms, we may view these spaces as spaces of piecewise smooth differential forms. They were in fact first constructed in this context, without any thought of finite elements or numerical methods, by Whitney [13]. The spaces were reinvented, one-by-one, as finite element spaces in response to the needs of various numerical problems, and the properties which are summarized in the commutative diagram above were slowly rediscovered as needed to analyze the resulting numerical methods. The connection between low order edge and face finite elements and Whitney forms was first realized by Bossavit [5].

Analogous statements hold for higher order Lagrange, edge, face, and discontinuous finite elements. For example, the following diagram commutes and has exact rows:

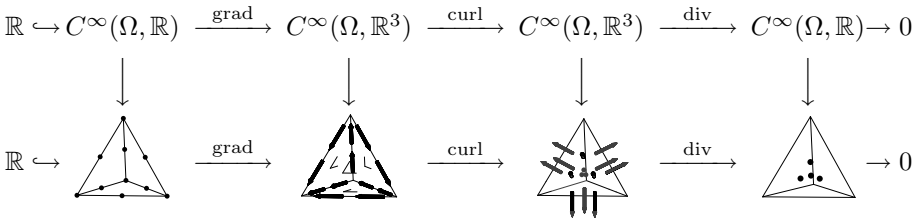

We shall see many other discrete differential complexes below.

4. Stability of Galerkin methods

Consider first the solution of the Dirichlet problem for Poisson's equation on a domain in $\mathbb{R}^n$:

$$-\Delta u = f \text{ in } \Omega, \quad u = 0 \text{ on } \partial\Omega.$$

The solution can be characterized as the minimizer of the energy functional

$$\mathcal{E}(u) := \frac{1}{2}\int_\Omega |\operatorname{grad} u(x)|^2\, dx - \int_\Omega f(x)u(x)\, dx$$

over the Sobolev space $\mathring{H}^1(\Omega)$ (consisting of $H^1(\Omega)$ functions vanishing on $\partial\Omega$), or as the solution of the weak problem: find $u \in \mathring{H}^1(\Omega)$ such that

$$\int_\Omega \operatorname{grad} u(x) \cdot \operatorname{grad} v(x)\, dx = \int_\Omega f(x)v(x)\, dx \quad \text{for all } v \in \mathring{H}^1(\Omega).$$

We may define an approximate solution u_h by minimizing the Dirichlet integral over a finite dimensional subspace W_h of $\mathring{H}^1(\Omega)$; this is the classical Ritz method. Equivalently, we may use the Galerkin method, in which $u_h \in W_h$ is determined by the equations

$$\int_\Omega \operatorname{grad} u_h(x) \cdot \operatorname{grad} v(x)\, dx = \int_\Omega f(x)v(x)\, dx \quad \text{for all } v \in W_h.$$

After choice of a basis in W_h this leads to a system of linear algebraic equations, and u_h is computable.

Let T_h denote the discrete solution operator $f \mapsto u_h$. Then it is easy to check that T_h is bounded as a linear operator from $H^{-1}(\Omega) := \mathring{H}^1(\Omega)^*$ to $\mathring{H}^1(\Omega)$ by a constant that depends only on the domain Ω (and, in particular, doesn't increase if the space W_h is enriched). This says that the Galerkin method is *stable*. A consequence is the *quasioptimality estimate*

$$\|u - u_h\|_{H^1} \le c \inf_{v \in W_h} \|u - v\|_{H^1}, \tag{4.4}$$

for some constant c depending only on the domain Ω. Note that there is no restriction on the subspace W_h to obtain this estimate. Galerkin's method for a coercive elliptic problem is always stable and convergence depends only on the approximation properties of the subspace. A natural choice for W_h is the Lagrange finite element space of some degree p with respect to some regular simplicial mesh of maximal element size h, in which case Galerkin's method is a standard finite element method. In this case the right hand side of (4.4) is $O(h^p)$ provided that u is sufficiently smooth.

Next consider the related eigenvalue problem, which arises in the determination of the fundamental frequencies of a drum. That is, we seek standing wave solutions $w(x,t)$ to the wave equation on some bounded domain $\Omega \subset \mathbb{R}^2$ which vanish on $\partial\Omega$. Assuming that the tension and density of the drum membrane are unity, these solutions have the form $w(x,t) = \alpha \cos(\sqrt{\lambda}t)u(x) + \beta \sin(\sqrt{\lambda}t)u(x)$ where α and β are constants and u and λ satisfy the eigenvalue problem

$$-\Delta u = \lambda u \text{ in } \Omega, \quad u = 0 \text{ on } \partial\Omega.$$

The eigenvalues λ form a sequence of positive numbers tending to infinity. The numbers $\sqrt{\lambda}/(2\pi)$ are the fundamental frequencies of the drum and the functions u give the corresponding fundamental modes.

The eigenvalues and eigenfunctions are characterized variationally as the critical values and critical points of the Rayleigh quotient

$$\mathcal{R}(u) = \frac{\int_\Omega |\operatorname{grad} u(x)|^2\, dx}{\int_\Omega |u(x)|^2\, dx},$$

defined for nonzero u belonging to the Sobolev space $\mathring{H}^1(\Omega)$. The classical Rayleigh–Ritz method for the approximation of eigenvalue problems determines approximate eigenvalues λ_h and eigenfunctions u_h as the critical values and points of the restriction of $\mathcal{R}$ to the nonzero elements of some finite dimensional subspace W_h of $\mathring{H}^1(\Omega)$. Equivalently, we can write the eigenvalue problem in weak form: find $\lambda \in \mathbb{R}$ and nonzero $u \in \mathring{H}^1(\Omega)$ such that

$$\int_\Omega \operatorname{grad} u(x) \cdot \operatorname{grad} v(x)\, dx = \lambda \int_\Omega u(x)v(x)\, dx \quad \text{for all } v \in \mathring{H}^1(\Omega). \tag{4.5}$$

The Galerkin approximation of the eigenvalue problem, which is equivalent to the Rayleigh–Ritz method, seeks $\lambda_h \in \mathbb{R}$ and nonzero $u_h \in W_h$ such that

$$\int_\Omega \operatorname{grad} u_h(x) \cdot \operatorname{grad} v(x)\, dx = \lambda_h \int_\Omega u_h(x)v(x)\, dx \quad \text{for all } v \in W_h. \tag{4.6}$$

We now discuss the convergence of this method. Let λ denote the jth eigenvalue of the problem (4.5). In the interest of simplicity we assume that λ is a simple eigenvalue, so the corresponding eigenfunction u is uniquely determined up to sign by the normalization $\|u\|_{H^1} = 1$. Similarly let λ_h and u_h denote the jth eigenvalue of (4.6). It can then be proved (see, e.g., [3] for much more general results) that there exists a constant c such that

$$\|u - u_h\|_{H^1} \le c \inf_{v \in W_h} \|u - v\|_{H^1}, \quad |\lambda - \lambda_h| \le c\|u - u_h\|^2_{H^1}. \tag{4.7}$$

In short, the eigenfunction approximation is quasioptimal and the eigenvalue error is bounded by the square. Again there is no restriction on the space W_h.

Figure 5 reports on the computation of the eigenvalues of the Laplacian on an elliptical domain of aspect ratio 3 using Lagrange finite elements of degree 1.

Now consider an analogous problem, the computation of the resonant frequencies of an electromagnetic cavity occupying a region $\Omega \subset \mathbb{R}^3$. In this case we wish to find standing wave solutions of Maxwell's equations. If we take the electric permittivity and the magnetic permeability to be unity and assume a lossless cavity with perfectly conducting boundary, we are led to the following eigenvalue problem for the electric field: find nonzero $E : \Omega \to \mathbb{R}^3$, $\lambda \in \mathbb{R}$ such that

$$\operatorname{curl}\operatorname{curl} E = \lambda E, \quad \operatorname{div} E = 0 \text{ in } \Omega, \quad E \times n = 0 \text{ on } \partial\Omega. \tag{4.8}$$

This is again an elliptic eigenvalue problem and the eigenvalues form a sequence of positive numbers tending to infinity. The divergence constraint is nearly redundant in this eigenvalue problem. Indeed if $\operatorname{curl}\operatorname{curl} E = \lambda E$ for $\lambda > 0$, then $\operatorname{div} E = \lambda^{-1} \operatorname{div}\operatorname{curl}\operatorname{curl} E = 0$ since the divergence of a curl vanishes. Thus the eigenvalue problem

$$\operatorname{curl}\operatorname{curl} E = \lambda E \text{ in } \Omega, \quad E \times n = 0 \text{ on } \partial\Omega, \tag{4.9}$$

has the same eigenvalues and eigenfunctions as (4.8) except that the it also admits $\lambda = 0$ as an eigenvalue, and the corresponding eigenspace is infinite-dimensional (it contains the gradients of all smooth functions vanishing on the boundary of Ω). The

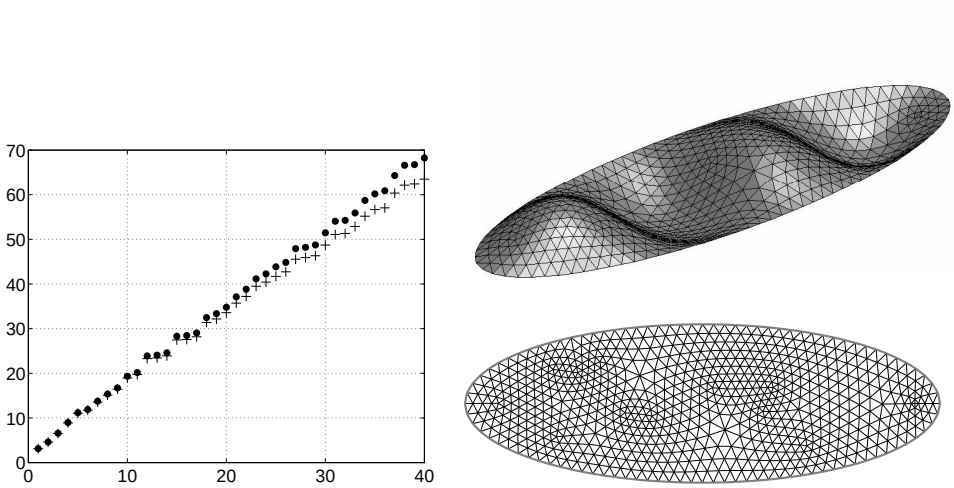

Figure 5: The point plot shows the first 40 eigenvalues computed with piecewise linear finite elements with respect to the triangulation shown (•) versus the exact eigenvalues (+). The surface plot shows the computed eigenfunction associated to the fourth eigenvalue. The mesh has 737 vertices, of which 641 are interior, and 1,376 triangles.

eigenvalues and eigenfunctions are now critical points and values of the Rayleigh quotient

$$\mathcal{R}(E) = \frac{\int_\Omega |\operatorname{curl} E(x)|^2 dx}{\int_\Omega |E(x)|^2 dx},$$

over the space of nonzero fields E in $\mathring{H}(\operatorname{curl}, \Omega)$, which is defined to be the space of functions for which both the above integrals exist and are finite and which have vanishing tangential component on the boundary (i.e., $E \times n = 0$ on $\partial\Omega$).

In Figure 6 we show the result of approximating a two-dimensional version of this eigenvalue problem using the Rayleigh–Ritz method or, equivalently, the Galerkin method with continuous piecewise linear vector fields on Ω whose tangential components vanish on the boundary (the first element depicted in Figure 3). For Ω we we take a square of side length π, in which case the nonzero eigenvalues are known to be all numbers of the form $\lambda = m^2 + n^2$ with $0 \leq m, n \in \mathbb{Z}$ not both zero, and the corresponding eigenfunctions are $E = (\sin my, \sin nx)$. For the mesh pictured, the finite element space has dimension 290. We find that 73 of the 290 computed eigenvalues are between 0 and 10 and that they have no tendency to cluster near the integers $1, 1, 2, 4, 4, 5, 5, 8, 9, 9$ which are the exact eigenvalues between 0 and 10. Thus this numerical method is useless: the computed eigenvalues bear no relation to the true eigenvalues! The analogue of (4.7) is surely not true.

If instead we choose the lowest order edge elements as the finite element space (Figure 3, top right), we get very different results. Using the same mesh, the edge finite element space has dimension 472. It turns out that 145 of the computed eigen-

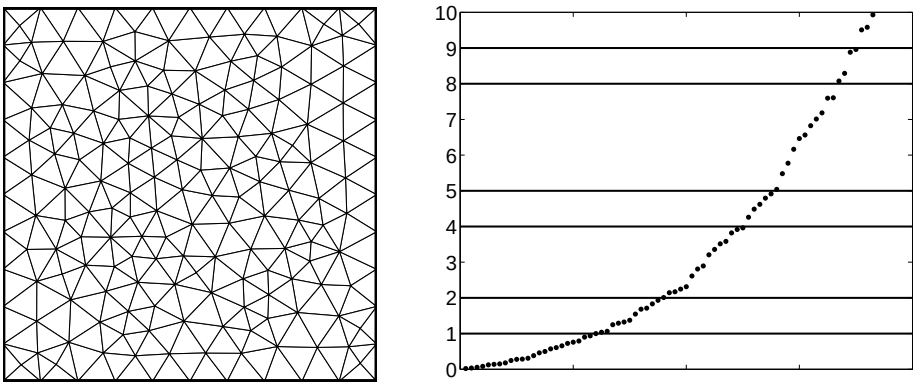

Figure 6: The plot shows the first 73 eigenvalues computed with piecewise linear finite elements for the resonant cavity problem on the square using the mesh shown. They bear no relation to the exact eigenvalues, 1, 1, 2, 4, 4, ..., indicated by the horizontal lines.

values are zero (to within round-off), and the subsequent eigenvalues are 0.9998, 0.9999, 2.0023, 3.9968, 4.0013, ..., i.e., excellent approximations of the exact eigenvalues. See Figure 7.

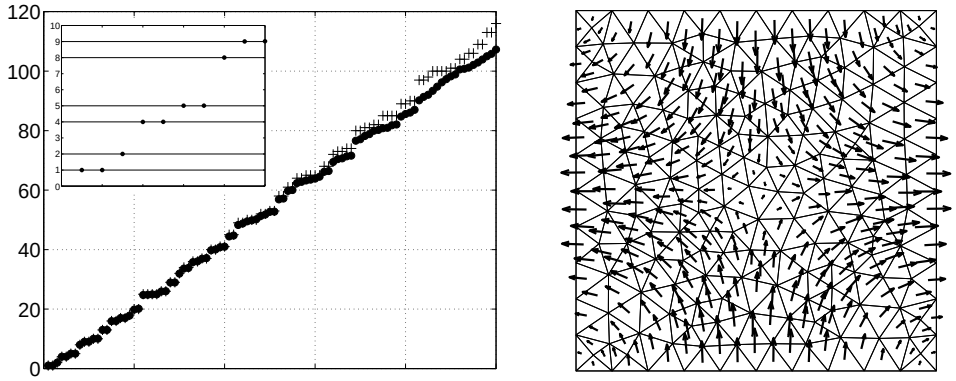

Figure 7: The first plot shows the first 100 positive eigenvalues for the resonant cavity problem on the square computed with lowest order edge elements using the mesh of Figure 6. The error in the first 54 eigenvalues is below 2%. The inset focuses on the first 10 eigenvalues, for which the error is less than 0.25%. The second plot shows the vector field associated to the third positive eigenvalue.

The striking difference between the behavior of the continuous piecewise linear finite elements and the edge elements for the resonant cavity problem is a question of stability. We shall return to this below, after examining stability in a simpler context.

5. Stability of mixed formulations

Consider now the Dirichlet problem

$$-\operatorname{div} C \operatorname{grad} u = f \text{ in } \Omega, \quad u = 0 \text{ on } \partial\Omega,$$

where Ω is a domain in $\mathbb{R}^3$ and the coefficient C is a symmetric positive definite matrix at each point. We may again characterize u as a minimizer of the energy functional

$$u \mapsto \frac{1}{2}\int C \operatorname{grad} u \cdot \operatorname{grad} u dx - \int f u \, dx$$

and use the Ritz method. This procedure is always stable.

However, for some purposes it is preferable to work with the equivalent first order system

$$\sigma = C \operatorname{grad} u, \quad -\operatorname{div} \sigma = f. \tag{5.10}$$

The pair (σ, u) is then characterized variationally as the unique critical point of the functional

$$\mathcal{L}(\sigma, u) = \int_\Omega (\frac{1}{2} C^{-1}\sigma \cdot \sigma + u \operatorname{div} \sigma) dx - \int_\Omega f u \, dx \tag{5.11}$$

over $H(\operatorname{div}, \Omega) \times L^2(\Omega)$. Note that (σ, u) is a saddle-point of $\mathcal{L}$, not an extremum. Numerical discretizations based on such saddle-point variational principles are called *mixed methods*.

It is worth interpreting the system (5.10) in the language of differential forms, because this brings some insight. The function u is a 0-form, and the operation $u \mapsto \operatorname{grad} u$ is just exterior differentiation. The vector field σ is a proxy for a 2-form and the operation $\sigma \mapsto \operatorname{div} \sigma$ is again exterior differentiation. The loading function f is the proxy for a 3-form. Since $\operatorname{grad} u$ is the proxy for a 1-form, it must be that the operation on differential forms that corresponds to multiplication by C takes 1-forms to 2-forms. In fact, if we untangle the identifications, we find that multiplication by C is a Hodge star operation. A Hodge star operator defines an isomorphism of $\bigwedge^k(\Omega)$ onto $\bigwedge^{3-k}(\Omega)$. To determine a particular such operator, we must define an inner product on the tangent space $\mathbb{R}^3$ at each point of Ω. The positive definite matrix C does exactly that. Many of the partial differential equations of mathematical physics admit similar interpretations in terms of differential forms. For a discussion of this in the context of discretization, see [9].

A natural approach to discretization of the mixed variational principle is to choose subspaces $S_h \subset H(\operatorname{div}, \Omega)$, $V_h \subset L^2(\Omega)$ and seek a critical point $(\sigma_h, u_h) \in S_h \times V_h$. This is of course equivalent to a Galerkin method and leads to a system of linear algebraic equations. However in this case, *stability is not automatic*. It can happen that the discrete system is singular, or more commonly, that the norm of the discrete solution operator grows unboundedly as the mesh is refined.

In a fundamental paper, Brezzi [6] established two conditions that together are sufficient (and essentially necessary) for stability. Brezzi's theorem applied to a wide class of saddle-point problems, but for simplicity we will state the stability conditions for the saddle-point problem associated to the functional (5.11).

(S1) There exists $\gamma_1 > 0$ such that

$$\int_\Omega C^{-1}\tau \cdot \tau \, dx \geq \gamma_1 \|\tau\|^2_{H(\mathrm{div})},$$

for all $\tau \in S_h$ such that $\int \mathrm{div}\, \tau \, v \, dx = 0$ for all $v \in V_h$.

(S2) There exists $\gamma_2 > 0$ such that for all $v \in V_h$ there exists nonzero $\tau \in S_h$ satisfying

$$\int_\Omega v \, \mathrm{div}\, \tau \, dx \geq \gamma_2 \|v\|_{L^2} \|\tau\|_{H(\mathrm{div})}.$$

Theorem (Brezzi) *If the stability conditions* (S1) *and* (S2) *are satisfied, then* $\mathcal{L}$ *admits a unique critical point* (σ_h, u_h) *over* $S_h \times V_h$*, the solution operator* $f \mapsto (\sigma_h, u_h)$ *is bounded* $L^2(\Omega) \to H(\mathrm{div}, \Omega) \times L^2(\Omega)$*, and the quasioptimal estimate*

$$\|\sigma - \sigma_h\|_{H(\mathrm{div})} + \|u - u_h\|_{L^2} \leq c \inf_{(\tau,v)\in S_h\times V_h} (\|\sigma - \tau\|_{H(\mathrm{div})} + \|u - v\|_{L^2})$$

holds with c *depending on* γ_1 *and* γ_2.

The stability conditions of Brezzi strongly limit the choice of the mixed finite element spaces S_h and V_h. Condition (S1) is satisfied if the indicated functions $\tau \in S_h$, those whose divergence is orthogonal to V_h, are in fact divergence-free. (In practice, this is nearly the only way it is satisfied.) This certainly holds if $\mathrm{div}\, S_h \subset V_h$, and so such as inclusion is a common design principle of mixed finite element spaces. On the other hand, condition (S2) is most easily satisfied if $\mathrm{div}\, S_h \supset V_h$, because in this case, given $v \in V_h$, we can choose $\tau \in S_h$ with $\mathrm{div}\, \tau = v$, so $\int_\Omega v \, \mathrm{div}\, \tau \, dx = \|v\|^2_{L^2}$, and the second condition will be satisfied as long as we can insure that $\|\tau\|_{H(\mathrm{div})} \leq \gamma_2^{-1} \|v\|_{L^2}$. In short, we need to know that div maps S_h onto V_h and that $\mathrm{div}\,|_{S_h}$ admits a bounded one-sided inverse.

The face elements of Raviart–Thomas and Nedelec were designed to satisfy both these conditions. Specifically, let S_h again denote the space of face elements of lowest degree (whose element diagram is shown in the middle of the second row of Figure 3), and V_h the space of piecewise constants.[1] We know that $S_h \subset H(\mathrm{div}, \Omega)$ so these elements are admissable for the mixed variational principle. Moreover, we have $\mathrm{div}\, S_h \subset V_h$, so (S1) holds.

To verify (S2), we refer to the commutative diagram (3.3). Given $v \in V_h$, we can solve the Poisson equation $\Delta\phi = v$ and take $\sigma = \mathrm{grad}\, \phi$ to obtain a function with $\mathrm{div}\, \sigma = v$ and $\|\sigma\|_{H^1} \leq C\|v\|_{L^2}$. Now let $\tau = \Pi^S_h \sigma \in S_h$. Then

$$\mathrm{div}\, \tau = \mathrm{div}\, \Pi^S_h \sigma = \Pi^V_h \, \mathrm{div}\, \sigma = \Pi^V_h v = v,$$

where we have used the commutativity and the fact that $v \in V_h$. Moreover $\|\tau\|_{H(\mathrm{div})} \leq c\|\sigma\|_{H^1} \leq c'\|v\|_{L^2}$, where we used the boundedness of Π^S_h on $H^1(\Omega, \mathbb{R}^3)$. This shows that $\mathrm{div}\, V_h = S_h$ and establishes a bound on the one-sided inverse, and

[1] It may seem odd to seek u_h in V_h, a space of discrete 3-forms, rather than in a space of 0-forms, since u is a 0-form. The resolution is through a Hodge star operator, this time formed with respect to the Euclidean inner product on $\mathbb{R}^3$. In the mixed method u_h is a discrete 3-form, approximating the image of u under this star operator.

so verifies (S2). Of course, the same argument shows the stability of a mixed method based on higher order face elements as well.

Thus we see that the stability of the mixed finite element method depends on the properties of the spaces V_h and S_h encoded in the rightmost square of the commutative diagram (3.3).

Now let us return to the resonant cavity eigenvalue problem (4.9) for which we explored the Galerkin method: find $\lambda_h \in \mathbb{R}$, $0 \neq E_h \in Q_h$ such that

$$\int_\Omega \operatorname{curl} E_h \cdot \operatorname{curl} F \, dx = \lambda_h \int_\Omega E_h \cdot F \, dx \quad \text{for all } F \in Q_h. \tag{5.12}$$

We saw that if $Q_h \subset \mathring{H}(\operatorname{curl}, \Omega)$ is taken to be a space of edge elements this method gives good results in that the positive eigenvalues of the discrete problem are good approximations for the positive eigenvalues of the continuous problem. However, the simple choice of Lagrange finite elements did not give good results. We now explain the good performance of the edge elements based on the middle square of the commutative diagram (3.3). Following Boffi et. al [4] we set $P_h = \operatorname{curl} Q_h$ and introduce the following mixed discrete eigenvalue problem: find $\lambda_h \in \mathbb{R}$, $0 \neq (E_h, p_h) \in Q_h \times P_h$ such that

$$\int_\Omega E_h \cdot F \, dx + \int_\Omega \operatorname{curl} F \cdot p_h \, dx = 0 \quad \text{for all } F \in Q_h, \tag{5.13}$$

$$\int_\Omega \operatorname{curl} E_h \cdot q \, dx = -\lambda_h \int_\Omega p_h \cdot q \, dx \quad \text{for all } q \in P_h. \tag{5.14}$$

It is then easy to verify that if λ_h, E_h is a solution to (5.12) with $\lambda_h > 0$, then λ_h, $(E_h, \lambda_h^{-1} \operatorname{curl} E_h)$ is a solution to (5.13), and if λ_h, (E_h, p_h) is a solution to (5.13) then $\lambda_h > 0$ and λ_h, E_h is a solution to (5.12). In short, the two problems are equivalent except that the former admits a zero eigenspace which the mixed formulation suppresses. As explained in [4], the accuracy of the mixed eigenvalue problem (5.13) hinges on the stability of the corresponding mixed source problem. This is a saddle-point problem of the sort studied by Brezzi, and so stability depends on conditions analogous to (S1) and (S2). The proof of these conditions in case Q_h is the space of edge elements follows, as in the preceding stability verification, from surjectivity and commutativity properties encoded in the diagram (3.3).

The diagram can also be used to explain the zero eigenspace computed with edge elements. Recall that in the case of the mesh shown in Figure 6, this space had dimension 145. In fact, this eigenspace is simply the null space of the curl operator restricted to Q_h. Referring again to the commutative diagram (3.3), this is the gradient of the space W_h of linear Lagrange elements vanishing on the boundary. Its dimension is therefore exactly the number of interior nodes of the mesh.

6. The elasticity complex

Let $\mathbb{S}$ denote the space of 3×3 symmetric matrices. Given a volumetric loading density $f : \Omega \to \mathbb{R}^3$, the system of linearized elasticity determines the displacement

field $u : \Omega \to \mathbb{R}^3$ and the stress field $\sigma : \Omega \to \mathbb{S}$ induced in the elastic domain Ω by the equations

$$\sigma = C\,\epsilon\,u, \quad -\operatorname{div}\sigma = f,$$

together with boundary conditions such as $u = 0$ on $\partial\Omega$. Here $\epsilon\,u$ is the symmetric part of the matrix $\operatorname{grad} u$, and the elasticity tensor $C : \mathbb{S} \to \mathbb{S}$ is a symmetric positive definite linear operator describing the particular elastic material, possibly varying from point to point.

The solution (σ, u) may be characterized variationally as a saddle-point of the Hellinger–Reissner functional

$$\mathcal{L}(\sigma, u) = \int_\Omega (\frac{1}{2} C^{-1}\sigma : \sigma + u \cdot \operatorname{div}\sigma) dx - \int_\Omega f \cdot u\, dx \tag{6.15}$$

over $H(\operatorname{div}, \Omega, \mathbb{S}) \times L^2(\Omega, \mathbb{R}^2)$ (i.e., σ is sought in the space of square-integrable symmetric-matrix-valued functions whose divergence by rows is square-integrable, and u is sought among all square-integrable vector fields).

For a mixed finite element method, we need to specify finite element subspaces $S_h \subset H(\operatorname{div}, \Omega, \mathbb{S})$ and $V_h \subset L^2(\Omega, \mathbb{R}^2)$ and restrict the domain of the variational problem. Of course the spaces must be carefully designed if the mixed method is to be stable: the analogues of the stability conditions (S1) and (S2) must be satisfied. The functional (6.15) is quite similar in appearance to (5.11) and so it might be expected that the mixed finite elements developed for the latter (the face elements for σ and discontinuous elements for u) could be adapted to the case of elasticity. In fact, the requirement of symmetry of the stress tensor and, correspondingly, the replacement of the gradient by the symmetric gradient, changes the structure significantly. Four decades of searching for mixed finite elements for elasticity beginning in the 1960s did not yield any stable elements with polynomial shape functions.

Using discrete differential complexes, R. Winther and the author recently developed the first such elements for elasticity problems in two dimensions [1]. (The three-dimensional case remains open.) For elasticity, the displacement and stress fields cannot be naturally interpreted as differential forms and the relevant differential complex is not the de Rham complex. In three dimensions it is instead the *elasticity complex*:

$$\mathbb{T} \hookrightarrow C^\infty(\Omega, \mathbb{R}^3) \xrightarrow{\epsilon} C^\infty(\Omega, \mathbb{S}) \xrightarrow{J} C^\infty(\Omega, \mathbb{S}) \xrightarrow{\operatorname{div}} C^\infty(\Omega, \mathbb{R}^3) \to 0.$$

Here the operator J is a *second order differential operator* which acts on a symmetric matrix field by first replacing each row with its curl and then replacing each column with its curl to obtain another symmetric matrix field. The resolved space $\mathbb{T}$ is the six-dimensional space of infinitesimal rigid motions, i.e., the same space of linear polynomials $a + b \times x$ which arose as the shape functions for the lowest order edge elements. If the domain Ω is topologically trivial, this complex is exact. Although it involves a second order differential operator, and so looks quite different from the de Rham complex, Eastwood [8] recently pointed out that it can be derived from the de Rham complex via a general construction known as the Bernstein–Gelfand–Gelfand resolution.

In two dimensions the elasticity complex takes the form

$$\mathbb{P}_1 \hookrightarrow C^\infty(\Omega) \xrightarrow{J} C^\infty(\Omega, \mathbb{S}) \xrightarrow{\text{div}} C^\infty(\Omega, \mathbb{R}^2) \to 0,$$

where now the second order differential operator is

$$J = \begin{pmatrix} \dfrac{\partial^2}{\partial x_2^2} & -\dfrac{\partial^2}{\partial x_1 \partial x_2} \\ -\dfrac{\partial^2}{\partial x_1 \partial x_2} & \dfrac{\partial^2}{\partial x_1^2} \end{pmatrix}.$$

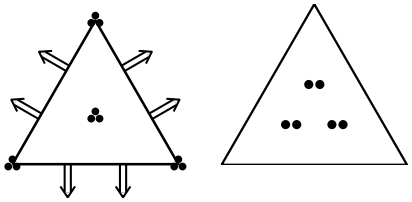

Figure 8: Element diagram for the new mixed finite elements for elasticity, lowest order case.

In the lowest order case, the finite elements we introduced in [1], for which the element diagrams can be seen in Figure 8, use discontinuous piecewise linear vector fields for the displacement field and a piecewise polynomial space which we shall now describe for the stress field. The shape functions on an arbitrary triangle T are given by

$$S_T = \{\, \tau \in \mathbb{P}_3(T, \mathbb{S}) \mid \operatorname{div} \tau \in \mathbb{P}_1(T, \mathbb{R}^2) \,\},$$

which is a 24-dimensional space consisting of all quadratic symmetric matrix fields on T together with the divergence-free cubic fields. The degrees of freedom are

- the values of three components of $\tau(x)$ at each vertex x of T (9 degrees of freedom)
- the values of the moments of degree 0 and 1 of the two components of τn on each edge e of T (12 degrees of freedom)
- the value of the three components of the moment of degree 0 of τ on T (3 degrees of freedom)

Note that these degrees of freedom are enough to ensure continuity of τn across element faces, and so will furnish a finite element subspace of $H(\text{div}, \Omega, \mathbb{S})$. The continuity is not however, the minimal needed for inclusion in $H(\text{div})$. The degrees of freedom also enforce continuity at the vertices, which is not required for membership in $H(\text{div})$. For various reasons, it would be useful to have a mixed finite element for elasticity that does not use vertex degrees of freedom. But, as we remark below, this is not possible if we restrict to polynomial shape functions.

In order to have a well-defined finite element, we must verify that the 24 degrees of freedom form a basis for the dual space of S_T. We include this verification since

it illustrates an aspect of the role of the elasticity complex. Since $\dim S_T = 24$, we need only show that if all the degrees of freedom vanish for some $\tau \in S_T$, then $\tau = 0$. Now τn varies cubically along each edge, vanishes at the endpoints, and has vanishing moments of degree 0 and 1. Therefore $\tau n \equiv 0$. Letting $v = \operatorname{div} \tau$, a linear vector field on T, we get by integration by parts that

$$\int_T v^2 \, dx = -\int_T \tau : \epsilon \, v \, dx + \int_{\partial T} \tau n \cdot v \, ds = 0$$

since the integral of τ vanishes as well as τn. Thus τ is divergence-free. In view of the exactness of the elasticity complex, $\tau = Jq$ for some smooth function q. Since all the second partial derivatives of q belong to $\mathbb{P}_3(T)$, $q \in \mathbb{P}_5(T)$. Adjusting by an element of $\mathbb{P}_1(T)$ (the null space of J), we may take q to vanish at the vertices. Now $\partial^2 q/\partial s^2 = \tau n \cdot n = 0$ on each edge, whence q is identically zero on ∂T. This implies that the gradient of q vanishes at the vertices. Since $\partial^2 q/\partial s \partial n = -\tau n \cdot t = 0$ on each edge (with t a unit vector tangent to the edge), we conclude that $\partial q/\partial n$ vanishes identically on ∂T as well. Since q has degree at most 5, it must vanish identically.

Let $\Pi_h^S : C^\infty(\Omega, \mathbb{S}) \to S_h$ denote the projection associated with the supplied degrees of freedom, and $\Pi_h^V : C^\infty(\Omega, \mathbb{R}^2) \to V_h$ the L^2-projection. For any triangle T, $\tau \in C^\infty(\Omega, \mathbb{S})$, and $v \in \mathbb{P}_1(\Omega, \mathbb{R}^2)$, we have

$$\int_T \operatorname{div}(\tau - \Pi_h^S \tau) \cdot v \, dx = -\int_T (\tau - \Pi_h^S \tau) : \epsilon \, v \, dx + \int_{\partial T} (\tau - \Pi_h^S \tau) n \cdot v \, ds.$$

The degrees of freedom entering the definition of Π_h^S ensure that the right hand side vanishes, and from this we obtain the commutativity $\operatorname{div} \Pi_h^S \tau = \Pi_h^V \operatorname{div} \tau$ which is essential for stability. (Actually a technical difficulty arises here, since Π_h^S as given is not bounded on $H^1(\Omega, \mathbb{S})$. See [1] for the resolution.) Note that, by their definitions, $\operatorname{div} S_h \subset V_h$ and, using the commutativity, we have $\operatorname{div} S_h = V_h$, i.e., $S_h \xrightarrow{\operatorname{div}} V_h \to 0$ is exact. To complete this to a discrete analogue of the elasticity complex, we define Y_h to be the inverse image of S_h under J. Then Y_h is exactly the space of C^1 piecewise quintic polynomials which are C^2 at the vertices of the meshes. This is in fact a well-known finite element space, called the Hermite quintic or Argyris space, developed for solving 4th order partial differential equations (for which the inclusion in $H^2(\Omega)$ and therefore C^1 continuity is required). The shape functions are $\mathbb{P}_5(T)$ and the 21 degrees of freedom are the values of the function and all its first and second partial derivatives at the vertices and the integrals of the normal derivatives along edges. We then have a *discrete elasticity complex*

$$\mathbb{P}_1 \hookrightarrow Y_h \xrightarrow{J} S_h \xrightarrow{\operatorname{div}} V_h \to 0,$$

or, diagrammatically,

$\mathbb{P}_1 \hookrightarrow$ 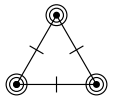 $\xrightarrow{J}$ 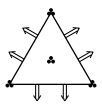 $\xrightarrow{\operatorname{div}}$ 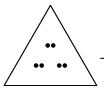 $\to 0.$

Moreover this sequence is exact and is coupled to the two-dimensional elasticity sequence via a commuting diagram:

$$\begin{array}{ccccccc}
\mathbb{P}_1 \hookrightarrow C^\infty(\Omega) & \xrightarrow{J} & C^\infty(\Omega,\mathbb{S}) & \xrightarrow{\text{div}} & C^\infty(\Omega,\mathbb{R}^3) & \to 0 \\
\downarrow \Pi_h^Y & & \downarrow \Pi_h^S & & \downarrow \Pi_h^V & \\
\mathbb{P}_1 \hookrightarrow Y_h & \xrightarrow{J} & S_h & \xrightarrow{\text{div}} & V_h & \to 0
\end{array}$$

The right half of this diagram encodes the information necessary to establish the stability of our mixed finite element method.

The Hermite quintic finite elements arose naturally from our mixed finite elements to complete the commutative diagram. Had they not been long known, we could have used this procedure to devise a finite element space contained in $H^2(\Omega)$. In fact, on close scrutiny we can see that any stable mixed finite elements for elasticity with polynomial shape functions will give rise to a finite element space with polynomial shape functions contained in $H^2(\Omega)$. However, it is known that such spaces are difficult to construct and complicated. In fact, it can be proved that an H^2 finite element space must utilize shape functions of degree at least 5 and the first and second partial derivatives at the vertices must be among the degrees of freedom [14]. This helps explain why mixed finite elements for elasticity have proven so hard to devise. In particular, we can rigorously establish the stress elements must involve polynomials of degree 3, and that vertex degrees of freedom are unavoidable.

In addition to the element just described, elements of all greater orders are also introduced in [1]. The elements of next higher order can be seen as the final two elements in this discrete elasticity complex.

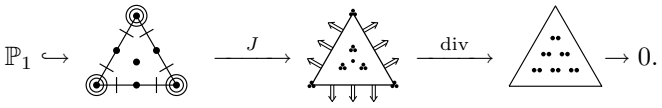

It is also possible to simplify the lowest order element slightly. To do this we reduce the displacement space from piecewise linear vector fields to piecewise rigid motions, and we replace the stress space with the inverse image under the divergence of the reduced displacement space. This leads to a stable element shown in this exact sequence:

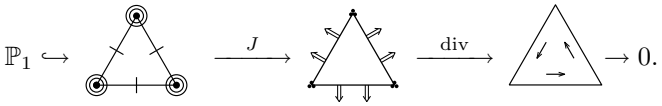

Because of the unavoidable complexity of H^2 finite elements, practitioners solving 4th order equations often resort to *nonconforming* finite element approximations of H^2. This means that the finite element space does not belong to H^2 in that the function or the normal derivative may jump across element boundaries, but the spaces are designed so that jumps are small enough in some sense (e.g., on average). The error analysis is more complicated for nonconforming elements, since

in addition to stability and approximation properties of the finite element space, one must analyze the *consistency error* arising from the jumps in the finite elements. In [2] Winther and the author investigated the the possibility of nonconforming mixed finite elements for elasticity, which, however are stable and convergent, and developed two such elements. These are related to nonconforming H^2 elements via nonconforming discrete elasticity complexes, two of which are pictured here:

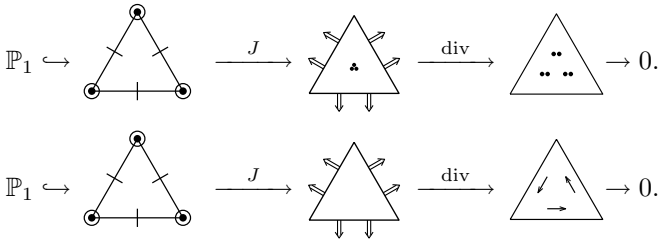

In both cases the shape function space for the stress is contained between $\mathbb{P}_1(T, \mathbb{S})$ and $\mathbb{P}_2(T, \mathbb{S})$. The nonconforming H^2 finite element depicted in these diagrams was developed for certain 4th order problems in [11]. Note the nonconforming mixed elasticity elements are significantly simpler than the conforming ones (and, in particular, don't require vertex degrees of freedom).

References

[1] D. N. Arnold & R. Winther, Mixed finite elements for elasticity, *Numer. Math.*, (2001).

[2] D. N. Arnold & R. Winther, Nonconforming mixed finite elements for elasticity, *Math. Models Methods Appl. Sci.*, to appear.

[3] I. Babuška & J. Osborn, Eigenvalue Problems, in: *Handbook of Numerical Analysis*, vol. II, P. G. Ciarlet & J. L. Lions, eds., Elsevier, 1991, pp. 641–788.

[4] D. Boffi, P. Fernandes, L. Gastaldi & I. Perugia, Computational models of electromagnetic resonators: analysis of edge element approximation, *SIAM J. Numer. Anal.*, 36 (1999), pp. 1264-1290.

[5] A. Bossavit, Whitney forms: a class of finite elements for three-dimensional computations in electromagnetism, *IEEE Proc. A*, 135 (1988), pp. 493–500.

[6] F. Brezzi, On the existence, uniqueness and approximation of saddle point problems arising from Lagrange multipliers, *Rev. Française Automat. Informat. Recherche Opérationnelle Sér. Rouge Anal. Numér.*, 8 (1974), pp. 129-151.

[7] P. G. Ciarlet, *The Finite Element Method for Elliptic Problems*, North-Holland, 1978.

[8] M. Eastwood, A complex from linear elasticity, *Rend. Circ. Mat. Palermo (2) Suppl.*, 63 (2000), pp. 23–29.

[9] R. Hiptmair, Finite elements in computational electromagnetism *Acta Numerica*, 11 (2002) 237–340.

[10] J.-C. Nedelec, Mixed finite elements in $\mathbb{R}^3$, *Numer. Math.*, 50 (1980), pp. 315–341.

[11] T. K. Nilsen, X.-C. Tai & R. Winther, A robust nonconforming H^2-element, *Math. Comp.*, 70 (2001), 489–505.
[12] P. A. Raviart & J. M. Thomas, A mixed finite element method for second order elliptic problems, Springer Lecture Notes in Mathematics vol. 606, Springer-Verlag, 1977, pp. 292–315.
[13] H. Whitney, *Geometric Integration Theory*, Princeton University Press, 1957.
[14] A. Ženišek, A general theorem on triangular $C^{(m)}$ finite elements, *Rev. Française Automat. Informat. Recherche Opérationnelle Sér. Rouge Anal. Numér.*, 8 (1974), pp. 119–127.